

Structure – Magnetism Relationships in α -Nitronyl Nitroxide Radicals

Mercè Deumal,^[a] Joan Cirujeda,^[b] Jaume Veciana,^{*[b]} and Juan J. Novoa^{*[a]}

Abstract: The crystal packing of α -nitronyl nitroxide radicals that have dominant ferromagnetic or antiferromagnetic interactions is analyzed in order to test if there are characteristic orientations of their functional groups that can be associated with these magnetic interactions. From a large crystalline structural database of compounds containing α -nitronyl nitroxide radical units (143 structures), 23 representative cases with dominant intermolecular ferromagnetic interactions, and 24 cases exhibiting dominant antiferromagnetic interac-

tions were selected. The spatial distribution of the N–O \cdots O–N, C(sp³)–H \cdots ON, and C(sp²)–H \cdots ON contacts whose distance is smaller than 10 Å was analyzed, with special emphasis on the 0–5 Å region for the N–O \cdots O–N contacts and 0–3.8 Å for the C–H \cdots O–N contacts. No correspondence is

found between the presence of intermolecular ferro- or antiferromagnetic interactions and the geometry of any of the previous isolated contacts. Therefore, there is a need to change the way in which some structure–magnetism correlations are obtained in α -nitronyl nitroxide crystals. These results also show that the intermolecular magnetic interaction is related to the relative orientation of the nearby molecules as a whole, that is, with the collection of intermolecular contacts made by them.

Keywords: crystal engineering • hydrogen bonds • magnetic properties • noncovalent interactions • radicals • solid-state structures

Introduction

The design of purely organic magnetic materials has been the goal of many research groups during the last decade.^[1] A systematic synthetic effort has provided different kinds of organic free radicals whose crystals present interesting magnetic properties, even bulk ferromagnetism in very exceptional cases.^[2] The most extensively studied family of purely organic persistent radicals are the α -nitronyl nitroxide (or α -nitronyl aminoxyl) radicals,^[3] whose general formula is shown at the top of Schemes 1 and 2.

The analysis of the magnetic properties and packing in the α -nitronyl nitroxide crystals shows that the presence of bulk ferromagnetism is strongly related to the relative disposition of the radicals in the crystal. This result is consistent with the commonly accepted theoretical models about intermolecular magnetism.^[1, 2, 4] For instance, the McConnell-I model,^[4] probably the one most employed today due to its simplicity,

predicts the presence of intermolecular ferromagnetic interactions between neighboring molecules only when there are short contacts between atoms that have a considerable atomic spin population of opposite sign (otherwise, the interaction would be antiferromagnetic or negligible).

The preparation of molecular organic crystals that show spontaneous magnetization below a certain critical temperature, T_C , is possible for persistent free radicals whose crystal packing allows for the presence of intermolecular ferromagnetic interactions propagating all over the crystal.^[5, 6] This is only possible if each spin containing molecule is capable of making one or more ferromagnetic interactions with its nearest neighbor molecules with strengths larger than kT_C , the thermal energy at T_C .^[7] Consequently, one of the most important points in this field is to recognize the relative arrangements of neighboring molecules giving rise to intermolecular ferromagnetic interactions, and those generating antiferromagnetic ones.^[8] Rationalization of the crystal packing of organic molecules can be achieved in terms of crystal-packing patterns,^[9] also known as synthons,^[10] the basic intermolecular units from which the rest of the crystal can be generated. Patterns for radical crystals with dominant ferromagnetic interactions can be called ferromagnetic patterns. Similarly antiferromagnetic patterns are these present in the crystals of radicals with dominant antiferromagnetic interactions.

The exact geometries of these patterns are still not known, a fact that has greatly limited the design of new organic magnets

[a] Prof. J. J. Novoa, Dr. M. Deumal
Departament de Química Física, Facultat de Química
Universitat de Barcelona
Av. Diagonal 647, E-08028 Barcelona (Spain)
Fax: (+34) 93-402-1231
E-mail: novoa@zas.qf.ub.es

[b] Dr. J. C. Cirujeda, Prof. J. Veciana
Institut de Ciència de Materials de Barcelona (CSIC)
Campus Bellaterra, E-08913 Cerdanyola (Spain)
Fax: (+34) 93-580-5729
E-mail: vecianaj@icmab.es

and the development of molecular magnetism. Up to now, the usual way of obtaining information about the structure of the ferro- and antiferromagnetic patterns has been by a detailed inspection of the molecular packing of individual crystals showing a well-characterized magnetic behavior. Although qualitative, several useful conclusions have been obtained using this methodology. For instance, it indicates that short $\text{NO}\cdots\text{ON}$ contacts are associated with antiferromagnetic patterns.^[1, 11, 12] Also, some short $\text{NO}\cdots\text{H}-\text{C}$ contacts are indicative of ferromagnetic patterns.^[1, 11, 12] This methodological approach has two major drawbacks: first of all, the structural information achieved on the magnetic patterns is very limited and, second, the conclusions are in many cases contaminated by preconceptions.^[13] Therefore, a systematic and quantitative analysis of the crystal packing of α -nitronyl nitroxides presenting dominant magnetic interactions is required to find their structure–magnetism relationships.

In this work we try to establish the presence of magnetic patterns by looking at the geometry of the $\text{N}-\text{O}\cdots\text{O}-\text{N}$ contacts, the most important magnetic ones according to the McConnell-I model, and also of the $\text{C}(\text{sp}^3)-\text{H}\cdots\text{ON}$ and $\text{C}(\text{sp}^2)-\text{H}\cdots\text{ON}$ contacts, given the claims of the presence of magnetic interactions through these hydrogen bonds.^[12] We have performed an analysis on 47 α -nitronyl nitroxide crystals that clearly show dominant ferromagnetic or antiferromagnetic intermolecular interactions; these were obtained from the literature or our own work.

Methodology

A total of 143 crystal structures containing substituted α -nitronyl nitroxide radical units were used initially. The majority were retrieved from the Cambridge Structural Database (CSD),^[14] and the rest from our own research, directly from the literature, or supplied by other authors. The criteria employed to select the final set of structures were as follows:

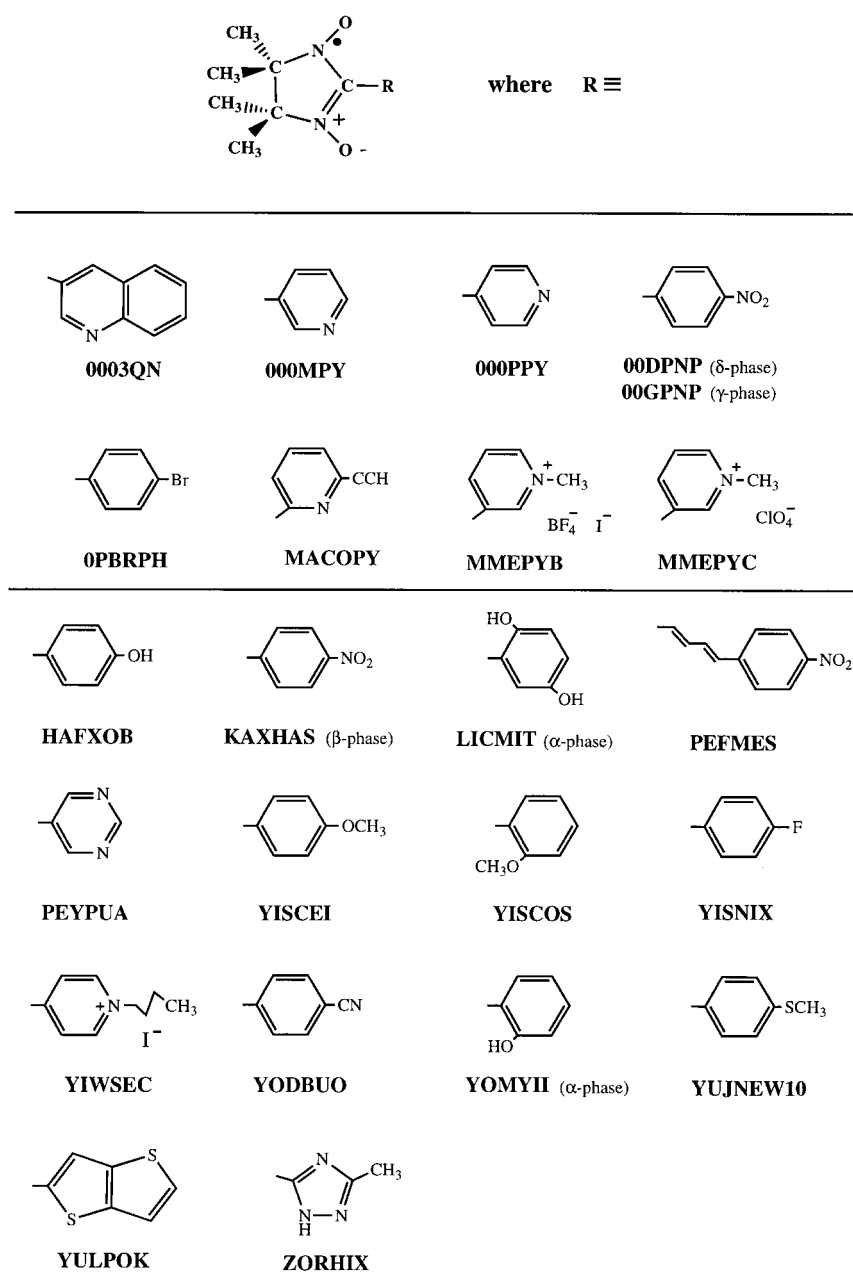
Abstract in Spanish: *Se ha analizado el empaquetamiento cristalino de los radicales α -nitronil nítróxido que presentan interacciones dominantes ferro o antiferromagnéticas, para ver si hay orientaciones de sus grupos funcionales características de cada tipo de interacción magnética. De entre un conjunto inicial de 143 cristales de radicales α -nitronil nítróxido, se seleccionan 23 casos con interacciones dominantes ferromagnéticas y 24 con interacciones dominantes antiferromagnéticas. La distribución espacial de los contactos $\text{N}-\text{O}\cdots\text{O}-\text{N}$, $\text{C}(\text{sp}^3)-\text{H}\cdots\text{ON}$ and $\text{C}(\text{sp}^2)-\text{H}\cdots\text{ON}$ cuya distancia es menor de 10 \AA se ha analizado, haciendo un énfasis especial en la región $0-5 \text{ \AA}$ para los contactos $\text{N}-\text{O}\cdots\text{O}-\text{N}$, y $0-3.8 \text{ \AA}$ para los $\text{C}-\text{H}\cdots\text{O}-\text{N}$. No se encuentra una relación entre la presencia de ferro o antiferromagnetismo y la geometría de ninguno de dichos contactos. Debido a ello, es necesario cambiar la forma en que se realizan muchas de las correlaciones magneto-estructurales en los cristales de radicales α -nitronil nítróxido. Estos resultados también muestran que las interacciones magnéticas intermoleculares están relacionadas con la orientación relativa de las moléculas vecinas como un todo, es decir, con el conjunto de contactos intermoleculares que producen entre ellas.*

1) The 26 structures with R factors greater than 0.10, or which were determined from very limited data, or which exhibit disorder or large molecular distortions, were discarded. 2) Then, the 45 structures containing both transition metal atoms and large closed-shell organic molecules cocrystallized were discarded (thus leaving 72 purely organic crystal structures), since intermolecular magnetic interactions between radicals could be complicated in these cases by the existence of other magnetic pathways through the metal atoms or the closed-shell molecules and the radical units. 3) Finally, we also discarded all the crystals whose magnetic interactions are not clearly dominated by ferro- or antiferromagnetic interactions.^[15] It is convenient to exclude all crystals with nondominating magnetic behavior because they can show both types of crystal packing patterns and, in consequence, it would make impossible the identification of the ferro- and antiferromagnetic patterns. The nature of the dominant magnetic interactions is clearly manifested by the temperature dependence of the magnetic susceptibility, χ , in the temperature range of $2-300 \text{ K}$.^[16] Radicals with dominant ferromagnetic interactions, grouped in the FM subset, show a characteristic continuous increase of χT as T decreases; radicals with dominant antiferromagnetic interactions have the opposite trend and were collected in the AFM subset. Of the remaining 47 purely organic crystals, 23 belonged to the FM subset^[17] and 24 to the AFM subset.^[18] The molecular structure of the parent radicals for each crystal is shown in Schemes 1 and 2.

Crystals whose structures were found in the CSD (27) are located in the lower part of both schemes. Under each drawing we have indicated the refcode given in the CSD database to the crystal (when more than one polymorph is present, all the refcodes are indicated). The equivalent information is provided in the upper part of Schemes 1 and 2 for the non-CSD crystals. In this case, an arbitrary refcode was generated by us for identification purposes and for compatibility with the crystal analysis codes. The 47 crystals of the combined FM and AFM subsets belong to the following space groups: $P\bar{1}$ (3), $P2_1$ (2), Cc (2), $P2_1/c$ (25), $C2/c$ (2), $P2_12_12_1$ (2), $Pca2_1$ (1), $Ib2a$ (1), $Pbca$ (4), $Fdd2$ (1), $I4_1/a$ (1), $P4_1bc$ (1), and $P3c1$ (2). Most of the analyzed crystal structures were determined at room temperature, where the thermal energy largely overcomes the strength of the magnetic interactions. Therefore, we are trying to correlate a physical property whose magnitude is only clearly observed at low temperatures, with the crystal packing at room temperature. This is a common practice in molecular magnetism that, unfortunately, cannot be avoided since only very few crystal structures have been determined at low temperatures. At first glance such objection may look serious, but a detailed analysis of this problem reveals that it has minor consequences for our magneto–structural correlations. Except for those cases where a first-order structural phase transition occur,^[19] the crystal packing patterns of molecular crystals show only small changes with the temperature due to the thermal contraction. These changes do not turn the relative disposition of the molecules (the data of interest here) to such an extent as to reverse the nature of the dominant intermolecular magnetic interaction.^[20] Therefore, it can be assumed without too much risk that the values of the distances and angles defining each contact would only change slightly with the temperature, and the differences in the geometrical distribution within the two subsets will still be of statistical significance.

One possible form of characterizing the relative positions of neighboring radicals is by looking at the relative geometry of the $\text{X}\cdots\text{Y}$ contacts which dominate the packing, together with those expected to give rise to the strongest magnetic interactions. Concerning the first type, the crystal packing of the α -nitronyl nitroxides is energetically dominated by the $\text{N}-\text{O}\cdots\text{O}-\text{N}$ and $\text{C}-\text{H}\cdots\text{O}-\text{N}$ contacts made among neighboring molecules.^[21, 22] On the other hand, according to the McConnell-I model, the dominant magnetic interactions present in the α -nitronyl nitroxide crystals are expected to be directly related to the spatial orientation and proximity of the ONCNO groups (these are the atoms in which most of the electronic spin distribution is located in the α -nitronyl nitroxide radicals).^[23] Therefore, we have investigated the statistical differences in the relative spatial dispositions of the $\text{N}-\text{O}\cdots\text{O}-\text{N}$ and $\text{C}-\text{H}\cdots\text{O}-\text{N}$ contacts within the FM and AFM subsets, searching for differences which later on could be used as signatures for the presence of a type of magnetic interaction in other α -nitronyl nitroxide crystals.

The statistical analysis of the geometry was done using the CSD module^[14] QUEST to locate the intermolecular contacts within each crystal, and the CSD-module VISTA for the visualization and a preliminary statistical treatment of the data. The CSD module PREQUEST was used to generate



Scheme 1. Chemical formulas of the R substituents for the α -nitronyl nitroxide radicals included in the FM subset. Lower part corresponds to those crystals whose structure has been deposited in the CSD.

structures suitable for their posterior treatment with QUEST for the non-CSD crystals. These crystal structures were added to the α -nitronyl nitroxide crystals recovered from the CSD. The factor and cluster analysis of the data were done with computer programs written in our laboratories. The number of intermolecular $\text{NO} \cdots \text{ON}$ and $\text{C-H} \cdots \text{O-N}$ contacts found in the 47 crystals of the combined FM and AFM is as follows: 1312 $\text{NO} \cdots \text{ON}$ contacts at $\text{O} \cdots \text{O}$ distances smaller than 10 Å, and 6039 $\text{C}(\text{sp}^3)\text{-H} \cdots \text{O-N}$ and 2286 $\text{C}(\text{sp}^2)\text{-H} \cdots \text{O-N}$ contacts at the same $\text{H} \cdots \text{O}$ cutoff. These three sets are large enough to allow a statistical analysis of the geometrical distribution of the parameters involved.

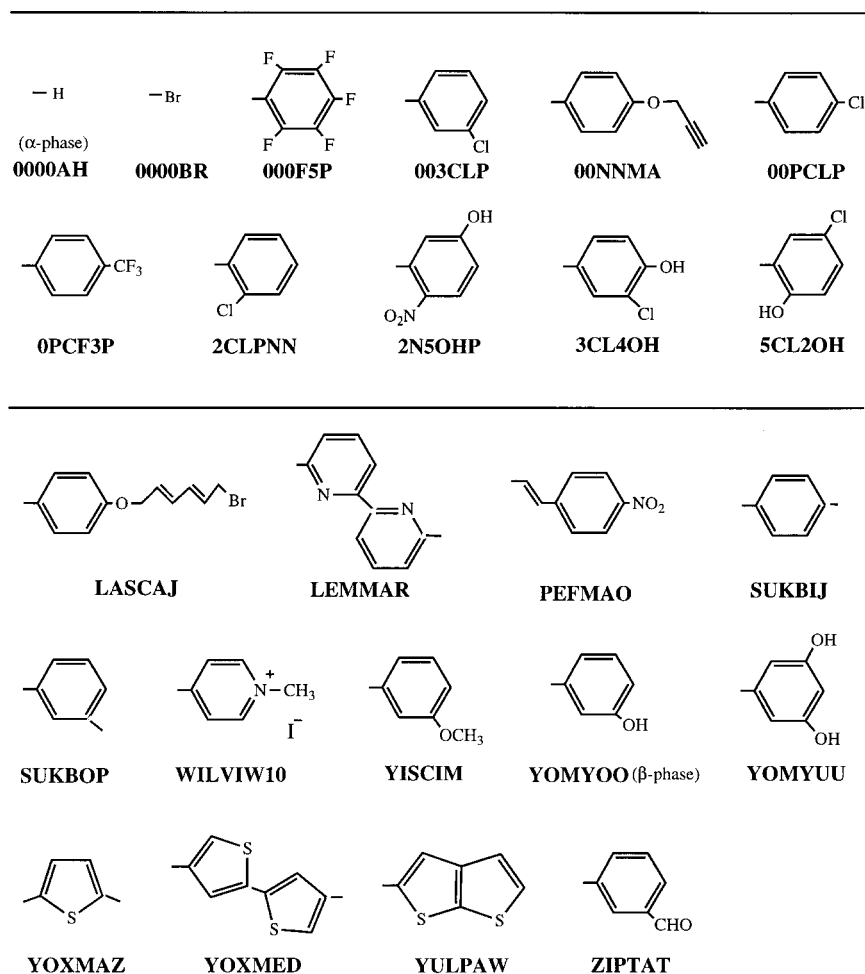
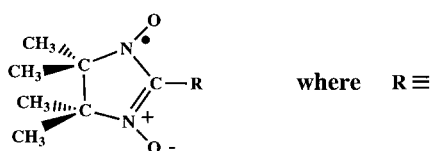
Results and Discussion

Spatial distributions of the $\text{N-O} \cdots \text{O-N}$ contacts: A preliminary statistical analysis of the geometry of the α -nitronyl nitroxide molecules of the 47 crystals included in the FM and

AFM subsets, and of other crystals with no definite, relevant, or complex magnetic behavior, showed that the spatial distribution of all the atoms present in the five-membered ring is nearly the same, and that the five ONCNO atoms lie in the same plane.^[24] This behavior can be attributed to the sp^2 hybridization of the α -C atom, which allows the delocalization of the π electrons over the five ONCNO atoms through various resonant forms. Given this fact, we do not have to worry about small distortions in the geometry of the ONCNO group and all the atoms of the imidazolidine ring, including the four methyl groups. Therefore, we can consider the internal geometry of imidazolidine ring and its ONCNO group as fixed. Consequently, given two ONCNO groups within a crystal, whose atoms are labeled as $\text{O}_{12}\text{N}_{12}\text{C}_1\text{N}_{11}\text{O}_{11}$ and $\text{O}_{22}\text{N}_{22}\text{C}_2\text{N}_{21}\text{O}_{21}$, the relative geometric position of the $\text{N}_{11}\text{-O}_{11} \cdots \text{O}_{21}\text{-N}_{21}$ contact is completely defined by the following six internal coordinates (see Figure 1): three to define the position of the terminal O_{21} atom relative to the $\text{O}_{12}\text{N}_{12}\text{C}_1\text{N}_{11}\text{O}_{11}$ group (the $\text{O}_{21} \cdots \text{O}_{11}$ distance, the $\text{O}_{21} \cdots \text{O}_{11}\text{-N}_{11}$ angle, and the $\text{O}_{21} \cdots \text{O}_{11}\text{-N}_{11}\text{-C}_1$ torsion angle), two for the position of the N_{21} atom for a fixed N-O distance ($\text{N}_{21}\text{-O}_{21} \cdots \text{O}_{11}$ angle and the $\text{N}_{21}\text{-O}_{21} \cdots \text{O}_{11}\text{-N}_{11}$ torsional angle), and one to fix the

$\text{O}_{22}\text{N}_{22}\text{C}_2\text{N}_{21}\text{O}_{21}$ group plane ($\text{C}_2\text{-N}_{21}\text{-O}_{21} \cdots \text{O}_{11}$ torsional angle, as the $\text{C}_2\text{-N}_{21}$ distance and the $\text{C}_2\text{-N}_{21}\text{-O}_{21}$ angle are fixed). To simplify the notation, we will identify these six parameters as D , A_1 , A_2 , T_1 , T_2 , and T_3 (see Figure 1). There are many other possible choices for this six coordinate space, but all of them are related by linear transformations. The coordinate set selected here is the one that allows an easier visualization and clearer physical interpretation of the geometric parameters.

The duplicities found during the geometric analysis of the contacts and the random spatial distributions of some angular parameters were taken into account by processing the geometrical data a) to discard those with nearly identical parameters, and b) to force the values of the angles A_1 and A_2 to be smaller than 180° and, at the same time, to impose



Scheme 2. Chemical formulas of the R substituents for the α -nitronyl nitroxide radicals included in the AFM subset. Lower part corresponds to those crystals whose structure has been deposited in the CSD.

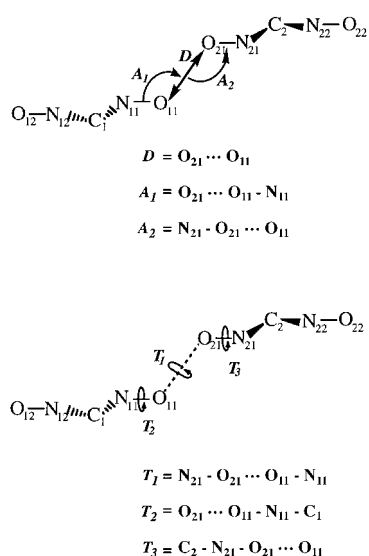


Figure 1. Geometrical parameters employed to define the relative position of two ONCNO groups.

that $A_1 \geq A_2$. This second condition was imposed because there is no way to force one ONCNO group to be the second group in the analysis carried out by using the QUEST program. No other restrictions were imposed in our data analysis.

We can begin the analysis of the geometry of the $NO \cdots ON$ contacts in the FM and AFM subsets by looking at their number as a function of the $O \cdots O$ distance (D parameter). There is a similar number of contacts in both subsets in the $0-n$ ($n \geq 10$) Å distance range analyzed (see Table 1). Such a long cutoff value is selected to allow the inclusion in our study of patterns in which the shortest contact between the neighboring molecules involves a bulky R substituent (like an aromatic ring) of one molecule and an O-N or other group of the second molecule. This forces the NO groups to lie far away.

The proportion of contacts in the FM and AFM subsets (see Table 1) is nearly constant for any cutoff distance within the $0-10$ Å range (on average, 44% are from the FM subset, with low and high values of 39% and 47%). These values suggest that the number of ONCNO \cdots ONCNO contacts that each NO group is making

is similar in both subsets. Consequently, it is not true that the presence of short $NO \cdots ON$ contacts is indicative of dominant antiferromagnetic interactions, as sometimes stated in the literature.^[1, 11, 12] This fact is better illustrated in Table 2, which

Table 1. List of ONCNO \cdots ONCNO contacts for crystals of the FM and AFM subsets within the range of distances indicated. Percentages of cases with intermolecular ferro- and antiferromagnetic interactions are also given.

distance range [Å]	total number of contacts	FM subset		AFM subset	
		number of contacts	%	number of contacts	%
[0-3]	0	0	0	0	0
[0-4]	24	10	42	14	58
[0-5]	92	36	39	56	61
[0-6]	204	90	44	114	56
[0-7]	378	167	44	211	56
[0-8]	608	274	45	334	55
[0-9]	901	416	46	485	54
[0-10]	1312	611	47	701	53

Table 2. Values of the geometrical parameters defining the ONCNO...ONCNO contact for the five crystals of the FM and AFM subsets showing the shortest D distances. The distances are given in Å and the angles in degrees. The refcodes of crystals in which these interactions are found are given in Schemes 1 and 2.

Refcode	D	A_1	A_2	T_1	T_2	T_3
FM subset						
LICMIT	3.158	146.8	146.8	180.0	-0.1	0.1
ZORHIX	3.168	126.9	71.5	119.0	46.5	-76.2
MMEPYC	3.429	153.2	68.0	173.3	-40.1	70.1
000MPY	3.499	127.5	76.4	-162.1	104.2	-92.1
PEYPUA	3.719	114.6	59.0	172.9	-114.0	-66.5
AFM subset						
WILVIW10	3.159	117.2	134.1	139.0	134.3	77.9
5CL2OH	3.369	82.6	82.6	180.0	75.6	-75.6
0000AH	3.431	120.0	75.8	-38.9	75.1	62.7
SUKBOP	3.522	77.7	77.7	180.0	-66.7	66.7
ZIPTAT	3.589	79.2	79.2	180.0	-82.7	82.7

gives the geometrical parameters of the FM and AFM crystals showing the shortest NO...ON contacts. Interestingly enough, the shortest NO...ON contact in the two subsets

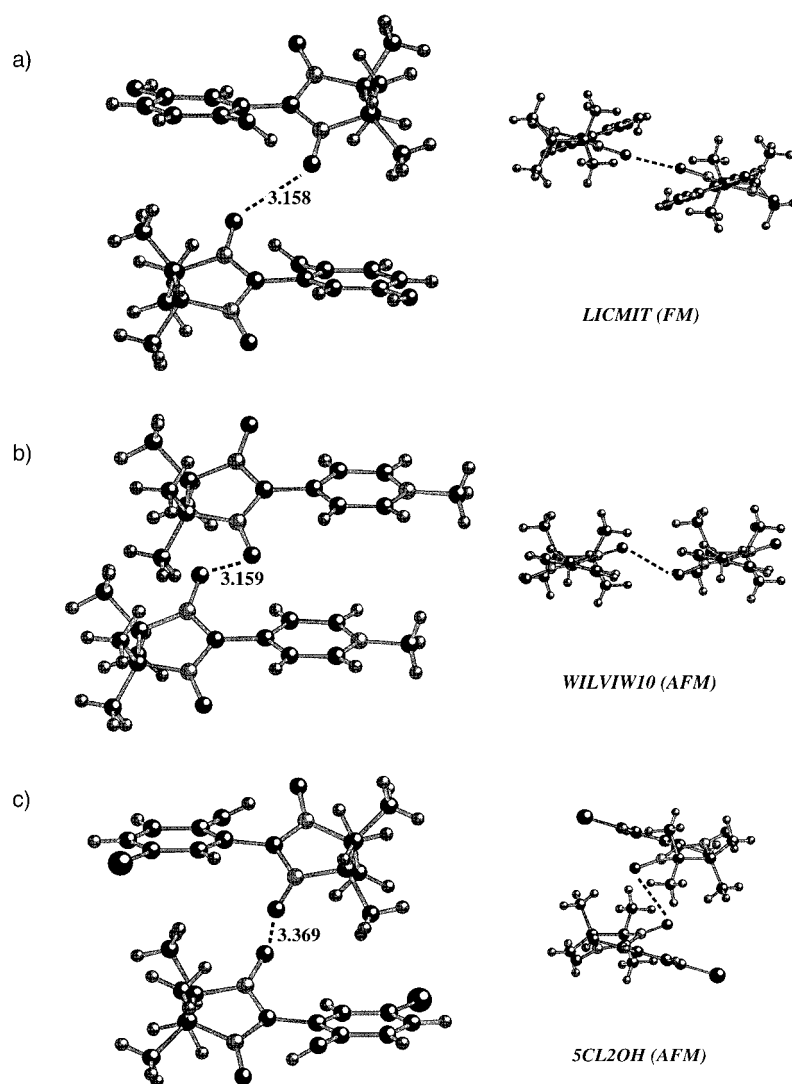


Figure 2. Geometrical disposition of the dimers found in the two crystals of the FM (a) and AFM subsets (b) presenting the shortest NO...ON contacts. Also shown (c) is the dimer with the shortest NO...ON contact among the dimers presenting a head-tail conformation in the AFM subset.

are nearly identical, 3.158 Å in the crystal of the FM subset and 3.159 Å in that of the AFM one (refcodes LICMIT and WILVIW10, respectively). Figure 2 shows the geometrical arrangement of the radicals in which these contacts are found. The arrangement is of the up-down type in the FM case and up-up type in the AFM case, but as it is also shown in Figure 2, there are also up-down arrangements within the AFM crystals presenting very short NO...ON contacts (Table 2). Thus, it is impossible to define the magnetic character of a crystal by looking only at the presence or absence of short NO...ON contacts.

We also performed a more detailed analysis evaluating the angular dependence. Comparing only the NO...ON distance distributions is like averaging the angular distribution for each distance value (see, for instance, the angle values given Table 2). Furthermore, as mentioned before, the McConnell-I model indicates that the angular orientation between nearby ONCNO groups is important to define the magnetic nature of the interaction. We first looked at the angular distribution in the FM and AFM subsets in the short end of our distance

analysis, the 3–5 Å range, as this is the most important region if the magnetic interaction is due to the direct overlap of the spin-density-containing groups (the NO groups). The scattergram of the values of D and T_2 for the FM and AFM subsets in the 3–10 Å region (Figure 3a) shows that there is a remarkable similarity in the two distributions along the 0–10 Å range. Scattergrams of other pairs of values show a similar behavior as that plotted in Figure 3a. To test if it is merely a consequence of the pair of parameters selected, we have also plotted (Figure 3b) the position of the O₂₁ atom relative to the N₁₁–O₁₁ group for all the contacts of the FM and AFM subsets within the 3–5 Å range. A direct observation of Figure 3b proves that: a) the O₂₁ atom is placed all over the space in the FM and AFM subgroups, and b) there is no difference between the spatial distributions of the FM and AFM subsets.

The similarity in the geometrical distribution of the FM and AFM N–O...O–N contacts is also found when the analysis is done in the 0–10 Å range. Similar scattergrams to those in Figure 3 are obtained, but with many more points. The similarity is clearly manifested by the average values of the parameters

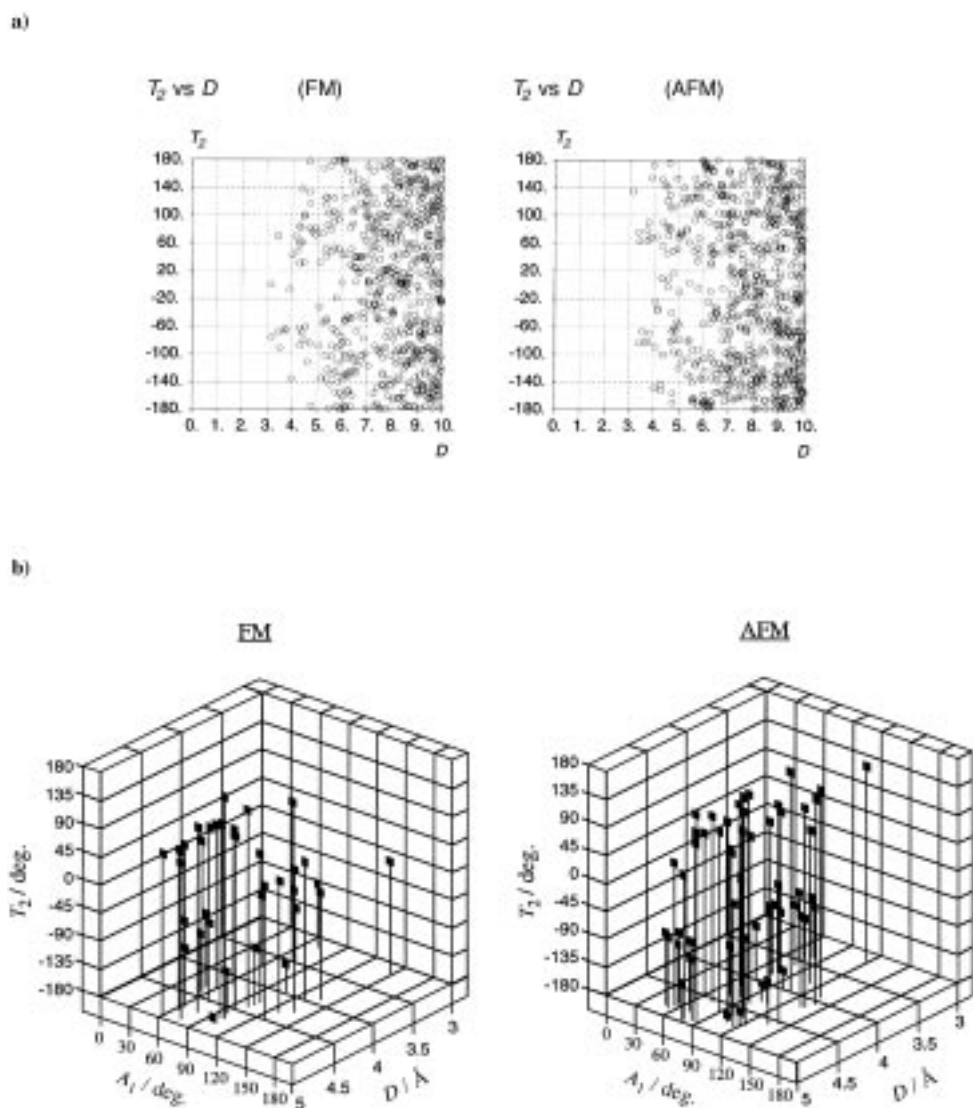


Figure 3. a) Scattergrams of the indicated pair of parameters characterizing the NO...ON contacts in the FM (left) and AFM (right) crystal subsets. b) Position of the O₂₁ atoms relative to the O₁₁-C₁₁-C₁ group for all contacts of the FM (left) and AFM (right) crystal subsets within the 0–5 Å range.

D , A_1 , A_2 , T_1 , T_2 , and T_3 . Within the 0–10 Å range, the average values of these parameters for the FM subset are 7.9 Å, 74°, 115°, 13°, 3°, and –5°, while the corresponding ones for the AFM subset are 7.8 Å, 73°, 113°, 8°, –6°, and 2°. These two sets of average values differ by less than their computed standard deviation.^[25] When the analysis was performed in the 0–4 Å range, the corresponding parameters also had similar average values for the FM and AFM subsets (in the same order as above, 3.6 Å, 92°, 137°, 18°, –22°, and –37° for the FM subset, and 3.6 Å, 88°, 93°, 32°, 44°, and 10° in the AFM subset). Once again, the FM and AFM average values differ by less than their standard deviation. Furthermore, the average value of the angular parameters found within the 0–4 and 0–10 Å ranges also differ by less than their standard deviation.

Therefore, even when the angular orientation is taken into account the presence of short NO...ON contacts does not imply that the crystal has dominant antiferromagnetic interactions. Consequently, one should change the way in which some magneto-structural analyses are done, as it is not

possible in general to define the nature of the dominant intermolecular magnetic interaction just by looking at the geometrical disposition of the closest NO...ON contacts.

Factor and cluster analysis of the geometry of the N–O...O–N contact:

At this point, we tested to see if the conclusions obtained in the previous section were due to the coordinate set employed, to inconsistencies or hidden trends in the data, or to the presence of hidden variables. To discard these options, one can perform a correlation and factor analysis of the data set, which consists of the geometries of the 611 and 701 ONCNO...ONCNO contacts found in the FM and AFM subsets, respectively.^[26, 27] As a final check we performed a cluster analysis, searching for possible clusters in the geometrical distribution of the six geometrical parameters, with the help of a well-defined mathematical procedure. This procedure allows the identification of particular regions in the relative orientation of the NO groups in which the ferro- or antiferromagnetic contacts are grouped, regardless of their strength. These regions would be associated with the existence of ferro- and/or antiferromagnetic interactions. For such a

cluster analysis, we considered the geometry of each contact as a six-component vector (V), each component being one of the six parameters employed to define the N–O...O–N contact geometry, that is, $V(1) = D$, $V(2) = A_1$, and so on. The values of the V components were renormalized to have a similar weight by giving the angles in radians.

As a first step, we investigated, independently in the FM and AFM subsets, our previous conclusions to see if they were a consequence of the coordinate set used in our study. The correlation matrix^[26] was then computed. In both subsets the off-diagonal elements always have an absolute value smaller than 0.17 (their average is 0.07 and 0.06 in the FM and AFM subsets), except for the A_1 and A_2 correlation, which has a value of 0.36. Therefore, there is a small correlation between the A_1 and A_2 angles, probably due to the tendency of many of these radicals to pack as stacks of planes.^[21, 22] No other correlation is found for any other pair of parameters employed in this study.

We also carried out a factor analysis^[27] of the 611×6 data matrix of the FM subset by computing the eigenvalues of the 6×6 covariance matrix, obtained from the data matrix by premultiplication by its transpose. The initial FM covariance matrix is nearly diagonal, thus indicating the linear independence of the coordinate set. Its eigenvalues are 4.096, 3.479, 3.246, 2.590, 0.374, and 0.177, the first three mostly associated to the three dihedral angles, the fourth to the distance D , and the last two to the A_1 and A_2 angles. Similar conclusions are found when the factor analysis is done on the AFM subset. Furthermore, in the AFM covariance matrix the eigenvalues and eigenvectors are nearly identical to those obtained in the FM subset, an indication of the similarity of their contacts, thus confirming our previous conclusions. In summary, these results indicate that six is the number of independent parameters needed in order to treat the NO...ON geometrical data. Therefore, the frequent use of three, or worse, two geometrical parameters when searching for structure-magnetism relationships is not correct.

As a final test on the validity of our data we carried out a cluster analysis^[28] of the ONCNO...ONCNO geometrical data. Specifically, we wanted to know whether the ONCNO...ONCNO contacts of the FM and AFM subsets are located in different regions of the six dimensional coordinate space. As a clustering criterion we used the single linkage method,^[28] also known as the nearest neighbor technique. Within this criterion, a cluster is defined as a set of connected elements, and one element i is said to be connected to its nearest neighbor j when the distance between both elements, d_{ij} ^[29] is equal or smaller than a threshold value, ϵ , that is, $d_{ij} \leq \epsilon$. This is a direct connection. If the element j is also connected to another element k , then i and k are indirectly connected and the cluster is constituted by the elements i , j , and k . Thus, a new element l is added to this cluster when the shortest distance to any element of the cluster is smaller than the threshold ϵ , a parameter which characterizes the cluster. If two clusters A and B are present in our data, they are characterized by two internal threshold values ϵ_A and ϵ_B , and the shortest distance between the elements of cluster A and cluster B must be larger than any of these two thresholds (see the upper part of Figure 4 for a graphical illustration).

To test if there are clusters of FM and/or AFM geometries, we applied the cluster analysis to the combined subsets of geometries. One can foresee three possible extreme situations, shown in Figure 4. In the first one, the FM and AFM subsets of contacts are disjoint, that is, the two sets of crystals pack in totally different forms. In the second case, there are common elements shared by the FM and AFM subsets. In the third case, the two sets of contacts are totally interpenetrated and indistinguishable, in fact forming only one set. As illustrated in Figure 4, one can mathematically differentiate among these three situations by comparing the shortest distance within the FM and AFM subsets (ϵ_{FM} and ϵ_{AFM}), with the shortest distance between the pairs of elements, one from each subset ($\epsilon_{\text{FM-AFM}}$). The subset in which each point is included is also known. If $\epsilon_{\text{FM-AFM}} > \epsilon_{\text{FM}}$ and, simultaneously, $\epsilon_{\text{FM-AFM}} > \epsilon_{\text{AFM}}$ the two subsets are disjoint, while if any of these two conditions are not fulfilled there is an overlap between the two sets and it is not possible to find two subsets

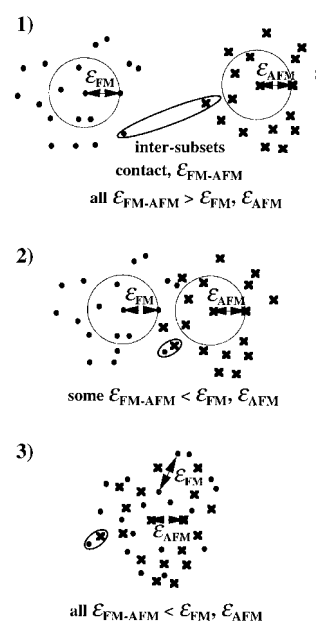


Figure 4. Types of clusters expected in our statistical analysis of FM and AFM subsets of crystals.

in a cluster analysis. One can differentiate between cases 2 and 3 mentioned above in the following way. The common elements between the FM and AFM subsets are those whose $\epsilon_{\text{FM-AFM}}$ is smaller than ϵ_{FM} and ϵ_{AFM} . If this number totals all the elements in the FM and AFM subsets, we are dealing with case 3, otherwise it is case 2.

The analysis of the FM and AFM geometrical data indicates that ϵ_{FM} and ϵ_{AFM} are 1.980 and 2.130, respectively. At the same time, $\epsilon_{\text{FM-AFM}} < \epsilon_{\text{FM}}$ and $\epsilon_{\text{FM-AFM}} < \epsilon_{\text{AFM}}$. Cluster analysis limited to NO...ON contacts shorter than 5 Å yielded the same conclusion as that done in the 0–10 Å region. Consequently, our sets of contacts are distributed according to the third possibility, that is, the two sets are nearly identical, interpenetrated, and indistinguishable. Thus, mathematically we find that there is no statistically significant difference in the relative disposition of the NO...ON contacts for the FM and AFM subsets. Notice here that the previous cluster analysis does not depend on the coordinate set employed, because the Cartesian distance between two vectors is invariant to the coordinate set in which these vectors are represented.

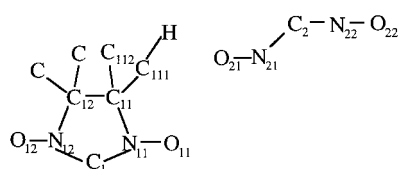
Spatial distributions of the $\text{C}(\text{sp}^3)\text{-H}\cdots\text{O-N}$ and $\text{C}(\text{sp}^2)\text{-H}$

...O-N contacts: The absence of a general connection between the geometry of the individual NO...ON contacts of neighboring molecules and the presence of dominant ferro- and antiferromagnetic interactions could be easily understood if there were other relevant magnetic interactions in the α -nitronyl nitroxide crystals. There have been some reports in the literature about the possibility of magnetic interactions through hydrogen bonds^[12] and the relevance of this implication in our crystals is obvious if one looks at Figure 2 for a while. Therefore, it is worthwhile to undertake the analysis of the distribution of hydrogen bonds in the α -nitronyl nitroxide crystals.

We focused our attention in the $\text{C}(\text{sp}^3)\text{-H}\cdots\text{O-N}$ and the $\text{C}(\text{sp}^2)\text{-H}\cdots\text{O-N}$ hydrogen bonds, as they constitute the majority of the H...O-N noncovalent interactions. The H

atoms of CH₃ and aromatic groups possess a small amount of spin.^[30] Therefore, accepting that the McConnell-I model can be extended to the H⋯O–N case, they are expected to give very weak magnetic interactions having a ferromagnetic nature when the spin density on the H atoms is negative and antiferromagnetic when it is positive.^[1, 4] Owing to their weakness, these kind of contacts are not expected to be the determinant ones in defining the dominant magnetic interaction in the crystal, although if their number is large enough, they could compensate the stronger ones. We have analyzed the geometry of all the C(sp³)–H⋯O–N and the C(sp²)–H⋯O–N contacts whose H⋯O distances are smaller or equal than 3.8 Å.^[31] This cutoff is longer than the usual one employed in the identification of hydrogen bonds, the reason being that the possible magnetic interactions generated through these bonds can be manifested at longer distances than these in which the hydrogen bonds present their minimum-energy distance, and we do not want to discard the presence of long-range magnetic contacts through hydrogen bonding.

A systematic search on the geometry of a general C–H⋯O–N contact requires six independent internal coordinates. However, given the quasi-cylindrical symmetry of the electron density around the C–H group, we can disregard two dihedrals and use the four parameters indicated in Figures 5



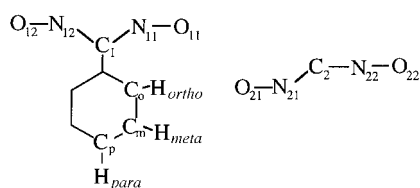
$$D = \text{H} \cdots \text{O}_{21}$$

$$A_1 = \text{H} \cdots \text{O}_{21} - \text{N}_{21}$$

$$A_2 = \text{C}_{111} - \text{H} \cdots \text{O}_{21}$$

$$T_1 = \text{C}_{111} - \text{H} \cdots \text{O}_{21} - \text{N}_{21}$$

Figure 5. Geometrical parameters employed to define the relative position of one C(sp³)–H group respect to a ONCNO group.



$$D_i = \text{H}_j \cdots \text{O}_{21}$$

$$A_{ii} = \text{H}_j \cdots \text{O}_{21} - \text{N}_{21}$$

$$A_{2i} = \text{C}_i - \text{H}_j \cdots \text{O}_{21}$$

$$T_{ii} = \text{C}_i - \text{H}_j \cdots \text{O}_{21} - \text{N}_{21}$$

$$(i = o, m, p)$$

$$(\text{H}_j = \text{H}_{ortho}, \text{H}_{meta}, \text{H}_{para})$$

Figure 6. Geometrical parameters employed to define the relative position of one C(sp²)–H group located in *ortho*, *meta* or *para* position of an aromatic ring respect to a ONCNO group.

and 6 for the C(sp³)–H⋯O–N and C(sp²)–H⋯O–N contacts, respectively. They will be called *D*, *A*₁, *A*₂, and *T*₁ for simplicity. In the C(sp²)–H⋯O–N case, one can distinguish between *ortho*, *meta*, and *para* C(sp²)–H⋯O–N contacts relative to the *α*-C atom of the five-membered ring. We have identified them by adding the suffix *o*, *m* and *p* and the name of the parameter (for instance *A*_{1o}, *A*_{1m} and *A*_{1p}).

All the crystals included in the two magnetic subsets have 12 hydrogen atoms bonded to the methyl C(sp³) atoms, which have a negative spin density.^[12a, 30] A proportion of 49% ferro- versus 51% antiferromagnetic C(sp³)–H⋯O–N contacts should be expected according to the number of crystals in the FM and AFM subsets. However, not all the crystals analyzed have functionalized aromatic groups in their *R* substituent (Schemes 1 and 2), and the proportion of ferro versus antiferromagnetic C(sp²)–H⋯O–N contacts will depend on the number of crystals having aromatic groups and on the number of hydrogens in *ortho*, *meta*, or *para* positions.

A search within the FM and AFM subsets for H⋯O distances smaller or equal to 3.8 Å^[31] gives 364 C(sp³)–H⋯

Table 3. Number of C(sp³)–H⋯ON and C(sp²)–H⋯ON contacts (split into *ortho*, *meta* and *para* contributions) within the FM and AFM subsets whose O⋯H distances are less or equal than 3.8 Å.

Type of contact	total number of contacts	FM subset		AFM subset	
		number of contacts	%	number of contacts	%
C(sp ³)–H⋯ON	364	157	43	207	57
C(sp ²)–H⋯ON					
<i>ortho</i>	35	20	57	15	43
<i>meta</i>	51	32	63	19	37
<i>para</i>	16	6	38	10	62

O–N contacts and 102 C(sp²)–H⋯O–N contacts, as indicated in Table 3, separated into *ortho*, *meta*, and *para* components. Within the 364 C(sp³)–H⋯O–N contacts, 43% belong to the FM subset and 57% to the AFM one, a similar proportion to the number of crystals in each subset. Similar proportions are found for the C(sp²)–H⋯O–N contacts in the FM and AFM subsets for hydrogens in the *ortho*, *meta*, and *para* positions. The contacts are distributed along *D* in a similar form for the FM and AFM subsets, as one can

Table 4. Values of the geometrical parameters defining the C(sp³)–H⋯O–N contacts for the five crystals of the FM and AFM subsets showing the shortest *D* distances. The distances are given in Å and the angles in degrees. The refcodes of crystals in which these contacts are found are also indicated.

Refcode	<i>D</i>	<i>A</i> ₁	<i>A</i> ₂	<i>T</i> ₁
FM subset				
HAFXOB	2.339	137.9	167.2	–145.3
YOMYII	2.382	111.9	162.2	94.9
000MPY	2.419	118.0	168.6	160.5
ZORHIX	2.582	126.8	148.1	169.2
00GPNP	2.600	124.1	132.1	–150.9
AFM subset				
0000AH	2.295	88.9	158.0	54.5
YISCIM	2.343	162.6	161.5	–109.3
SUKBIJ	2.442	142.1	161.2	–148.0
0000BR	2.447	126.3	149.6	112.3
YOXMED	2.489	131.3	157.7	–157.8

Table 5. Values of the geometrical parameters defining the C(sp²)–H...O–N contacts for the three crystals within the FM / AFM subsets showing the shortest contact distances. The values are grouped into three different sets according to the positions (*ortho*, *meta*, and *para*) of the H atoms that make the indicated contacts. The distances are given in Å and the angles in degrees. The refcodes of crystals in which these contacts are found are also indicated.

	Refcode	D_o	A_{1o}	A_{2o}	T_{1o}
FM	00GPNP	2.559	157.5	123.6	–103.3
	00DPNP	2.569	158.3	123.0	118.6
	KAXHAS	2.800	123.1	101.7	–82.7
AFM	SUKBOP	2.645	125.8	125.1	–134.5
	2N5OHP	2.698	101.6	124.9	–152.8
	YOMYUU	2.791	157.9	125.5	100.7
	Refcode	D_m	A_{1m}	A_{2m}	T_{1m}
FM	YISNIX	2.239	150.7	147.8	102.0
	00DPNP	2.421	132.4	130.6	–143.7
	HAFXOB	2.496	143.0	128.1	–171.9
AFM	0PCF3P	2.412	140.6	137.0	120.9
	3CL4OH	2.647	143.2	127.9	–95.0
	YOMYOO	2.648	153.5	145.2	–131.9
	Refcode	D_p	A_{1p}	A_{2p}	T_{1p}
FM	YOMYII	2.613	135.1	163.3	–92.0
	LICMIT	2.892	139.2	127.4	88.1
	YISCOS	2.940	112.3	118.4	156.6
AFM	5CL2OH	2.220	137.0	157.0	–95.6
	YISCIM	2.325	148.2	142.7	–157.6
	003CLP	2.465	152.3	127.7	179.6

appreciate by comparing the values for the shortest contacts in the two subsets in Tables 4 and 5. One always finds C(sp³)–H...O–N contacts in the FM and AFM subsets, irrespective of the range analyzed (for instance, there are 2 FM and 2 AFM C(sp³)–H...O–N contacts in [2.2–2.4] range, and similar numbers are found for the C(sp²)–H...O–N contacts), although the percentage of FM versus AFM can change a bit with the range (for instance, if the cutoff is for 3.0 Å 65% of the C(sp³)–H...O–N contacts are in the FM subset). The presence of C(sp³)–H...O–N contacts in both subsets at all ranges does not depend on the H...O cutoffs or range employed. All of this is clearly manifested in the scattergrams shown in Figures 7 and 8.

A more complete idea of the distribution of these contacts in space requires the inclusion of the angular distribution. We can do so by means of the scattergrams of Figures 7 and 8, which represent views of the

values of the D , A_1 , and A_2 parameters for the C–H...O–N contacts in the two magnetic subsets. Similar behavior is found when one looks at other pairs of parameters. Although the number of points in Figures 7 and 8 is not large enough to allow generalizations, the C(sp²)–H...O–N contacts are distributed in a similar way for the FM and AFM subsets, within the 80–180° range, for the angles, and the 2.2–3.8 Å range for the distances. The use of cutoffs shorter than 3.8 Å does not change our conclusions. Thus, we can conclude that no differences are found in the geometrical distribution of the C–H...O–N contacts of the FM and AFM subsets.

Conclusion

Our analysis indicates that there are no statistically significant differences in the relative disposition of the NO...ON and C–H...O–N contacts found within the FM and AFM subsets. This experimental observation is consistent with the fact that the packing of α -nitronyl nitroxide radicals is driven by the same intermolecular forces in the FM and AFM crystals. Consequently, it is not possible to determine the nature (ferro- or antiferromagnetic) of the dominant magnetic interaction in a crystal just by looking at the geometry of one type of intermolecular contact. This assertion breaks some accepted ideas, such as the association of the dominant

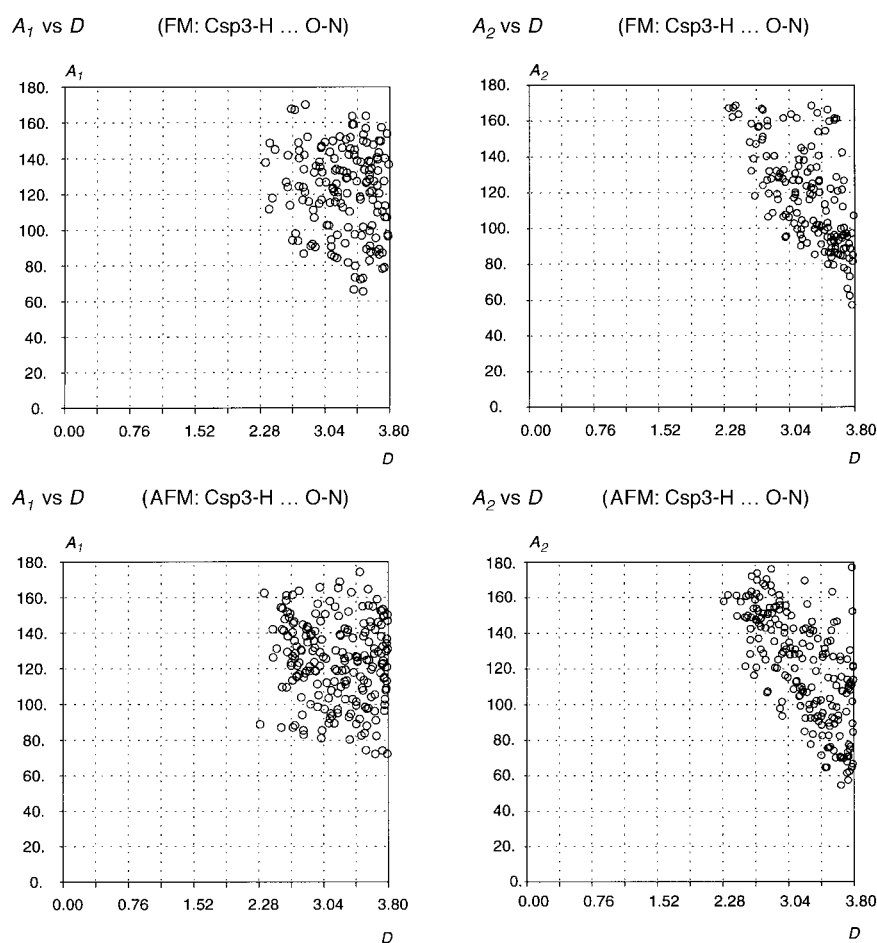


Figure 7. Scattergrams of A_1 vs. D and A_2 vs. D for the C(sp³)–H...O–N contacts of the FM (upper) and AFM (lower) subsets.

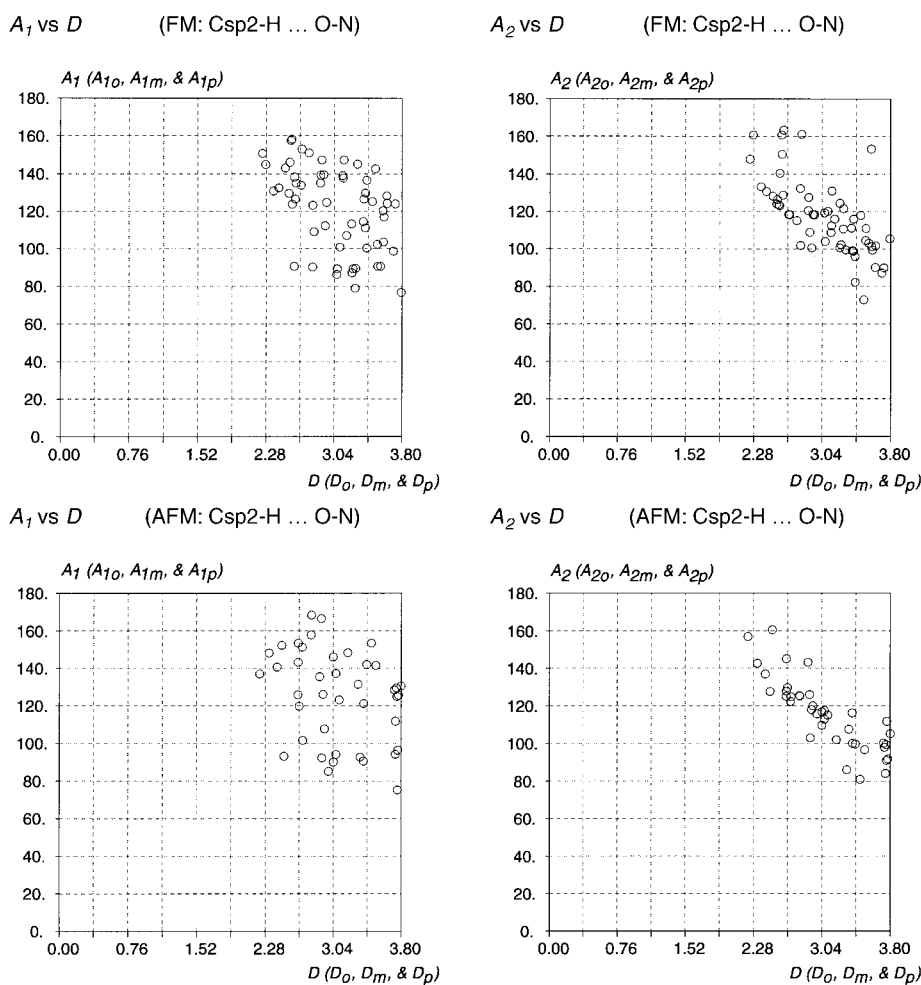


Figure 8. Scattergram of A_1 vs. D and A_2 vs. D for the *ortho*, *meta*, and *para* $C(sp^2)-H \cdots O-N$ contacts of the FM (upper) and AFM (lower) subsets.

magnetic character of a crystal with the presence of short $NO \cdots ON$ distances. We have also found that six is the number of independent parameters needed to represent the $NO \cdots ON$, thus invalidating the frequent use of three or two geometrical parameters when searching for structure–magnetism relationships.

Now we need to address an interesting point: if the crystals of a magnetic subset must have dominant interactions of its subset class, and these interactions clearly depend on the relative geometrical arrangement of the radicals, why are these differences not seen in the previous statistical analysis? Two different answers can be given to this question. First, the McConnell-I model might not be valid and could be just an oversimplification of the experimental operative mechanism.^[32] Second, it could be that we have looked at individual intermolecular connections, assuming that magnetism in these solids is associated to the relative position of an *individual* contact, while the experimental intermolecular interactions are *collective*, that is, associated to the relative disposition of *all* magnetically active functional groups. The second idea can be illustrated by looking at the differences in the packing patterns of Figure 2: the relative orientations of the $NO \cdots ON$ contacts are not so different in these geometrical arrangements, but the geometrical dispositions of the molecules and all the functional groups in the molecule is very different (that

is, one is dealing with different packing patterns). Our statistical study does not rule out any of these options and further studies are necessary for such a task.^[33]

Acknowledgments

This work was supported by the DGES (Project PB95-0848-C02-02 and PB96-0862-C02-01) and CIRIT (Projects GRP94-1077 and GRQ93-8028). M.D. and J.C. acknowledge CIRIT for their doctoral grants. The authors also thank Prof. M. Kinoshita (U. Tokyo), Prof. O. Kahn (Bordeaux), Dr. P. Rey (Grenoble), Dr. K. Awaga (U. Tokyo), and Dr. T. Sugawara (U. Tokyo) for providing us with some preliminary crystal data. We would like also to thank Dr. S. Motherwell (CCDC, Cambridge) for providing us access to a beta version of the PRE-QUEST program and for the help provided in using it. We also thank Dr. D. Amabilino for manuscript revision and valuable comments.

[1] For a recent overview see:

- a) *Molecular Magnetic Materials* (Eds.: D. Gatteschi, O. Kahn, J.-S. Miller, F. Palacio), Kluwer Academic, Dordrecht, **1991**; b) *Mol. Cryst. Liq. Cryst.* (Eds.: H. Iwamura, J.-S. Miller) **1993**, 232/233, pp. 1–360/1–366; c) J.-S. Miller, A.-J. Epstein, *Angew. Chem.* **1994**, 33, 399; *Angew. Chem. Int. Ed. Engl.* **1994**, 33, 385; d) O. Kahn, *Molecular Magnetism*, VCH, New York, **1993**; e) A. Rajca, *Chem. Rev.* **1994**, 94, 871; f) J.-S. Miller, A.-J. Epstein, *Mol. Cryst. Liq. Cryst.* **1995**, 272–274; g) M. Kinoshita, *Jpn. J. Appl. Phys.* **1994**, 33, 5718; h) *Molecular Magnetism: From Molecular Assemblies to Devices* (Eds.: E. Coronado, P. Delhaes, D. Gatteschi, J.-S. Miller), Kluwer Academic, Dordrecht, **1996**; i) *Magnetism: A Supramolecular Function* (Ed.: O. Kahn), Kluwer Academic, Dordrecht, **1996**; j) *Mol. Cryst. Liq. Cryst.* (Eds.: K. Itoh, J. S. Miller, T. Takui), **1997**, 305/306, pp. 1–586/1–520.
- [2] a) M. Tamura, Y. Nakazawa, D. Shiomi, K. Nozawa, Y. Hosokoshi, M. Ishikawa, M. Takahashi, M. Kinoshita, *Chem. Phys. Lett.* **1991**, 186, 401; b) P.-M. Allemand, K.-C. Khemani, A. Koch, F. Wudl, K. Holzer, S. Donovan, G. Grüner, J.-D. Thompson, *Science*, **1991**, 253, 301; c) R. Chiarelli, M.-A. Novak, A. Rassat, J.-L. Tholance, *Nature*, **1993**, 363, 147; d) T. Sugawara, M.-M. Matsushita, A. Izuoka, N. Wada, N. Takeda, M. Ishikawa, *J. Chem. Soc. Chem. Commun.* **1994**, 1081; e) J. Cirujeda, M. Mas, E. Molins, F. Lanfranc de Panthou, J. Laugier, J. Geun Park, C. Paulsen, P. Rey, C. Rovira, J. Veciana, *J. Chem. Soc. Chem. Commun.* **1995**, 709; f) A. Caneschi, F. Ferraro, D. Gatteschi, A. LeLirzin, M.-A. Novak, E. Rentscheler, R. Sessoli, *Adv. Mater.* **1995**, 7, 476; g) Y. Pei, O. Kahn, M.-A. Aebersold, L. Ouahab, F. Le Berre, L. Pardi, J.-L. Tholance, *Adv. Mater.* **1994**, 6, 681; h) K. Togashi, K. Imachi, K. Tomioka, H. Tsuboi, T. Ishida, T. Nogami, N. Takeda, M. Ishikawa, *Bull. Chem. Soc. Jpn.* **1996**, 69, 2821, and references therein.
- [3] α -Nitronyl nitroxide is the abbreviated name most widely employed, it is used here to indicate 4,5-dihydro-4,4,5,5-tetramethyl-3-oxido-1H-imidazol-3-ium-1-oxyl, the correct IUPAC name.

- [4] H.-M. McConnell, *J. Chem. Phys.* **1963**, *39*, 1910.
- [5] In general, bulk ferromagnetism requires the presence of ferromagnetic interactions along three (or two) directions of the solid, depending on whether there is a low (or high) magnetic anisotropy. Since organic free radicals in general have very small magnetic anisotropy, the presence of ferromagnetic interactions in three dimensions is required for achieving bulk ferromagnetism. See: F. Palacio, *From Ferromagnetic Interactions to Molecular Ferromagnets: An Overview of Models and Materials* (Eds.: D. Gatteschi, O. Kahn, J.-S. Miller, F. Palacio, in *Magnetic Molecular Materials*), Kluwer Academic, Dordrecht, **1991**, pp. 1–40.
- [6] A lack of compensation of the magnetic moments of spins coupled antiferromagnetically can also produce a net magnetic moment—spin canting—that, when propagated over the solid, produces a spontaneous magnetization. For a recent organic example of this situation, see: A.-J. Banister, N. Bricklebank, I. Lavender, J.-M. Rawson, C.-I. Gregory, B.-K. Tanner, W. Clegg, R. R. J. Elsegood, F. Palacio, *Angew. Chem.* **1996**, *108*, 2648; *Angew. Chem. Int. Ed. Engl.* **1996**, *35*, 2533.
- [7] For molecular organic crystals with high symmetry, namely cubic, the presence of just one intermolecular ferromagnetic interaction among the neighboring units is enough in order to guarantee the propagation of magnetic interactions along two or three spatial directions. By contrast, for crystals with lower symmetries there must be more than one intermolecular ferromagnetic interaction for each crystallographically independent radical molecule in order to achieve a bulk ferromagnetism.
- [8] Another important aspect to be developed in this field is the enhancement of the strengths of intermolecular magnetic interactions. On increasing these strengths it will be possible to increase the critical temperature of purely organic ferromagnets, which nowadays are still very low; most of them in the mK region.
- [9] M.-C. Etter, *Acc. Chem. Res.* **1990**, *23*, 120; J. Bernstein, R.-E. Davis, L. Shimoni, N.-L. Chang, *Angew. Chem.* **1995**, *107*, 1689; *Angew. Chem. Int. Ed. Engl.* **1995**, *34*, 1555.
- [10] G. Desiraju, *Angew. Chem.* **1995**, *107*, 2541; *Angew. Chem. Int. Ed. Engl.* **1995**, *34*, 2311.
- [11] For example see: a) K. Awaga, T. Inabe, Y. Maruyama, T. Nakamura, M. Matsumoto, *Chem. Phys. Lett.* **1992**, *195*, 21; b) K. Awaga, T. Inabe, T. Nakamura, M. Matsumoto, Y. Maruyama, *Mol. Cryst. Liq. Cryst.* **1993**, *232*, 69; c) K. Awaga, T. Okuno, A. Yamaguchi, M. Hasegawa, T. Inabe, Y. Maruyama, N. Wada, *Phys. Rev. B* **1994**, *49*, 3975.
- [12] For example see: a) J. Veciana, J. Cirujeda, C. Rovira, J. Vidal-Gancedo, *Adv. Mater.* **1995**, *7*, 221; b) J. Cirujeda, E. Hernández, C. Rovira, J.-L. Stanger, P. Turek, J. Veciana, *J. Mater. Chem.* **1995**, *5*, 243; c) M. M. Matsushita, A. Izuoka, T. Sugawara, T. Kobayashi, N. Wada, N. Takeda, M. Ishikawa, *J. Am. Chem. Soc.* **1997**, *119*, 4369.
- [13] When no angular data are taken into account and only intermolecular distances are considered in a given magnetostructural correlation, one is always tempted to ascribe the observed ferromagnetic intermolecular interaction to the contacts between atoms of the two interacting molecules that have opposite spin densities and are at the closest distances. However, in some molecular layouts there could be other atoms at longer distances that interact ferromagnetically due to angular considerations.
- [14] F.-H. Allen, S. Bellard, M.-D. Brice, B.-A. Cartwright, A. Doubleday, H. Higgs, T. Hummelink, B.-G. Hummelink-Peters, O. Kennard, W. D. S. Motherwell, J.-R. Rodgers, D.-G. Watson, *Acta Crystallogr. Sect. B* **1979**, *35*, 2331.
- [15] When the magnetic susceptibility data show the typical signature of the presence of two competing ferro- and antiferromagnetic interactions, we considered that one of them is dominant only when its strength—deduced by the fitting of magnetic data to different magnetic models—is at least one order of magnitude larger than the other one. In cases with comparable magnitudes we discarded the crystal structure from our statistical analysis.
- [16] In few cases magnetic susceptibility data down only to 4 K are available.
- [17] The 23 ferromagnetic crystals selected are listed and are identified by their refcode and reference (when the crystal is not deposited in the Cambridge Structural Database we have assigned a refcode and indicate the source): 0003QN: T. Sugano, M. Tamura, M. Kinoshita, Y. Sakai, Y. Ohashi, *Chem. Phys. Lett.* **1992**, *200*, 235; 000MPY: F. Lanfranc de Panthou, PhD Thesis, Univ. J. Fourier Grenoble I, **1994**; 000PPY: K. Awaga, T. Inabe, Y. Maruyama, *Chem. Phys. Lett.* **1992**, *190*, 349; 00DPNP: Prof. M. Kinoshita, unpublished results; 00GPNP: P. Turek, K. Nozawa, D. Shiomi, K. Awaga, T. Inabe, Y. Maruyama, M. Kinoshita, *Chem. Phys. Lett.* **1991**, *180*, 327; 0PBRPH: Y. Hosokoshi, PhD Thesis, Univ. of Tokyo, **1995**; MACOPY: F. M. Romero, R. Ziessel, A. De Cian, J. Fischer, P. Turek, *New J. Chem.* **1996**, *20*, 919; MMEPYB: K. Awaga, T. Inabe, Y. Maruyama, T. Nakamura, M. Matsumoto, *Chem. Phys. Lett.* **1992**, *195*, 21; MMEPYC: K. Awaga, T. Okuno, A. Yamaguchi, M. Hasegawa, T. Inabe, Y. Maruyama, N. Wada, *Phys. Rev. B* **1994**, *49*, 3975; HAFXOB: E. Hernández, M. Mas, E. Molins, C. Rovira, J. Veciana, *Angew. Chem.* **1993**, *105*, 919; *Angew. Chem. Int. Ed. Engl.* **1993**, *32*, 882; KAXHAS: K. Awaga, T. Inabe, U. Nagashima, Y. Maruyama, *J. Chem. Soc. Chem. Commun.* **1989**, 1617; LICMIT: T. Sugawara, M.-M. Matsushita, A. Izuoka, N. Wada, N. Takeda, M. Ishikawa, *J. Chem. Soc. Chem. Commun.* **1994**, 1723; PEFMES: H. Wang, D. Zhang, M. Wan, D. Zhu, *Solid State Commun.* **1993**, *85*, 685; PEYPUA: F. Lanfranc de Panthou, D. Luneau, J. Laugier, P. Rey, *J. Am. Chem. Soc.* **1993**, *115*, 9095; YISCEI: L. Angeloni, A. Caneschi, L. David, A. Fabretti, F. Ferraro, D. Gatteschi, A. le Lirzin, R. Sessoli, *J. Mater. Chem.* **1994**, *4*, 1047; YISCOS: L. Angeloni, A. Caneschi, L. David, A. Fabretti, F. Ferraro, D. Gatteschi, A. le Lirzin, R. Sessoli, *J. Mater. Chem.* **1994**, *4*, 1047; YISNIX: Y. Hosokoshi, M. Tamura, M. Kinoshita, H. Sawa, R. Kato, Y. Fujiwara, Y. Ueda, *J. Mater. Chem.* **1994**, *4*, 1219; YIWSEC: K. Awaga, A. Yamaguchi, T. Okuno, T. Inabe, T. Nakamura, M. Matsumoto, Y. Maruyama, *J. Mater. Chem.* **1994**, *4*, 1377; YODBUO: Y. Hosokoshi, M. Tamura, H. Sawa, R. Kato, M. Kinoshita, *J. Mater. Chem.* **1995**, *5*, 41; YOMYII: J. Cirujeda, M. Mas, E. Molins, F. Lanfranc de Panthou, J. Laugier, J. Geun Park, C. Paulsen, P. Rey, C. Rovira, J. Veciana, *J. Chem. Soc. Chem. Commun.* **1995**, 709; YUJNEW10: A. Caneschi, F. Ferraro, D. Gatteschi, A. le Lirzin, E. Rentschler, *Inorg. Chim. Acta* **1995**, *235*, 159; YULPOK: T. Akita, Y. Mazaki, K. Kobayashi, N. Koga, H. Iwamura, *J. Org. Chem.* **1995**, *60*, 2092; ZORHIX: A. Lang, Y. Pei, L. Ouahab, O. Kahn, *Adv. Mater.* **1996**, *8*, 60.
- [18] The 24 antiferromagnetic crystals selected are listed and are identified by their refcode and reference (when the crystal is not deposited in the Cambridge Structural Database we have assigned a refcode and indicate the source): 0000AH: Y. Hosokoshi, PhD Thesis, Univ. of Tokyo, **1995**; 0000BR: Y. Hosokoshi, PhD Thesis, Univ. of Tokyo, **1995**; 000F5P: Y. Hosokoshi, PhD Thesis, Univ. of Tokyo, **1995**; 003CLP: O. Jürgens, J. Cirujeda, M. Mas, I. Mata, A. Cabrero, J. Vidal-Gancedo, C. Rovira, E. Molins, J. Veciana, *J. Mater. Chem.* **1997**, *7*, 1723; 00NNMA: E. Hernández, PhD Thesis, Univ. of Barcelona, **1995**; 00PCLP: Y. Hosokoshi, PhD Thesis, Univ. of Tokyo, **1995**; 0PCF3P: Y. Hosokoshi, PhD Thesis, Univ. of Tokyo, **1995**; 2CLPNN: O. Jürgens, J. Cirujeda, M. Mas, I. Mata, A. Cabrero, J. Vidal-Gancedo, C. Rovira, E. Molins, J. Veciana, *J. Mater. Chem.* **1997**, *7*, 1723; 2N5OHP: J. Cirujeda, PhD Thesis, Univ. Ramon Llull, **1997**; 3CL4OH: O. Jürgens, J. Cirujeda, M. Mas, I. Mata, A. Cabrero, J. Vidal-Gancedo, C. Rovira, E. Molins, J. Veciana, *J. Mater. Chem.* **1997**, *7*, 1723; 5CL2OH: O. Jürgens, J. Cirujeda, M. Mas, I. Mata, A. Cabrero, J. Vidal-Gancedo, C. Rovira, E. Molins, J. Veciana, *J. Mater. Chem.* **1997**, *7*, 1723; LASCAJ: D. Zhang, W. Zhou, D. Zhu, *Solid State Commun.* **1993**, *86*, 291; LEMMAR: D. Luneau, J. Laugier, P. Rey, G. Ulrich, R. Ziessel, P. Legoll, M. Drillon, *J. Chem. Soc. Chem. Commun.* **1994**, 741; PEFMAO: H. Wang, D. Zhang, M. Wan, D. Zhu, *Solid State Commun.* **1993**, *85*, 685; SUKBIJ: A. Caneschi, P. Chiesi, L. David, F. Ferraro, D. Gatteschi, R. Sessoli, *Inorg. Chem.* **1993**, *32*, 1445; SUKBOP: A. Caneschi, P. Chiesi, L. David, F. Ferraro, D. Gatteschi, R. Sessoli, *Inorg. Chem.* **1993**, *32*, 1445; WILVIW10: K. Awaga, A. Yamaguchi, T. Okuno, T. Inabe, T. Nakamura, M. Matsumoto, Y. Maruyama, *J. Mater. Chem.* **1994**, *4*, 1377; YISCIM: L. Angeloni, A. Caneschi, L. David, A. Fabretti, F. Ferraro, D. Gatteschi, A. le Lirzin, R. Sessoli, *J. Mater. Chem.* **1994**, *4*, 1047; YOMYOO: J. Cirujeda, M. Mas, E. Molins, F. Lanfranc de Panthou, J. Laugier, J. Geun Park, C. Paulsen, P. Rey, C. Rovira, J. Veciana, *J. Chem. Soc. Chem. Commun.* **1995**, 709; YOMYUU: J. Cirujeda, M. Mas, E. Molins, F. Lanfranc de Panthou, J. Laugier, J. Geun Park, C. Paulsen, P. Rey, C. Rovira, J. Veciana, *J. Chem. Soc. Chem. Commun.* **1995**, 709; YOXMMAZ: T. Mitsumori, K. Inoue, N. Koga, H. Iwamura, *J. Am. Chem. Soc.* **1995**, *117*, 2467; YOXMED: T. Mitsumori, K. Inoue, N. Koga, H. Iwamura, *J.*

- Am. Chem. Soc.* **1995**, *117*, 2467; YULPAW: T. Akita, Y. Mazaki, K. Kobayashi, N. Koga, H. Iwamura, *J. Org. Chem.* **1995**, *60*, 2092; ZIPTAT: A. Caneschi, D. Gatteschi, E. Rentschler, R. Sessoli, *Gazzetta Chim. Ital.* **1995**, *125*, 283.
- [19] Such first-order transitions generally produce abrupt changes in the χT versus T plots that are easily detected.
- [20] This fact has been well documented for organic superconducting crystals, whose critical temperatures are also much lower than the room temperature. See, for instance, J.-M. Williams, J.-R. Ferraro, R.-J. Thorn, K.-D. Carlson, U. Geiser, H.-H. Wang, A.-M. Kini, M.-H. Whangbo, *Organic Superconductors*, Prentice Hall, Englewood Cliffs, **1992**. Magnetism is a different physical property than superconductivity, although both are intimately related with the relative arrangement of molecules in the crystal. The packing properties of molecular solids and, in particular, its variation with temperature, are determined by the intermolecular contacts, but is independent of the electronic physical properties of the crystal.
- [21] J. Veciana, J. Cirujeda, C. Rovira, E. Molins, J.-J. Novoa, *J. Phys. I* **1996**, *6*, 1067.
- [22] a) M. Deumal, J. Cirujeda, J. Veciana, M. Kinoshita, Y. Hosokoshi, J.-J. Novoa, *Chem. Phys. Lett.* **1997**, *265*, 190; b) J. J. Novoa, M. Deumal, M. Kinoshita, Y. Hosokoshi, J. Veciana, J. Cirujeda, *Mol. Cryst. Liq. Cryst.* **1997**, *305*, 129.
- [23] The presence of a positive density on the O atom has been shown by experimental and theoretical methods. See for instance, A. Zheludev, V. Barone, M. Bonnet, B. Delley, A. Grand, E. Ressouche, P. Rey, R. Subra, J. Schweizer, *J. Am. Chem. Soc.* **1994**, *116*, 2019; J.-J. Novoa, F. Mota, J. Veciana, J. Cirujeda, *Mol. Cryst. Liq. Cryst.* **1995**, *271*, 79.
- [24] Standard deviations of the atomic distances and bond angles of this five-membered ring are smaller than the 2% of the respective magnitudes. See: J. Cirujeda, PhD. Thesis, Univ. Ramon Llull, Barcelona, **1997**.
- [25] The standard deviation of the geometrical parameters for the FM and AFM subsets are also similar. Their values are larger for the angles than the distance D , and, among the angles, are larger for the T_i than the A_i parameters. This trend just reflects the softer form of the potential energy curves of the dihedral parameters, compared with the angles and distance stretchings.
- [26] R. Barlow, *Statistics*, Wiley, Chichester, **1989**.
- [27] E.-R. Malinowski, D.-G. Howery, *Factor Analysis in Chemistry*, Wiley Interscience, New York, **1980**.
- [28] B.-S. Everitt, *Cluster Analysis*, 3rd ed., Edward Arnold, London, **1993**.
- [29] The distance between two elements, i and j , in the space defined by six dimensional coordinates space is given by Equation (1).
- $$d_{ij} = \sum_{k=1}^6 [V(k)_i^2 - V(k)_j^2]^{1/2} \quad (1)$$
- [30] The spin density on the H atom of the four CH₃ groups is negative, whereas these on the H atoms of a phenyl ring linked to the α carbon of the five membered ring alternate in their sign, being positive for *ortho* and *para* H atoms and negative for the *meta* one. See: ref. [23].
- [31] A distance range not much longer than that used in recent analysis of C–H...O hydrogen bonded contacts to avoid excluding the so-called outliers. See: G. A. Jeffrey, W. Saenger, *Hydrogen Bonding in Biological Structures*, Springer, Berlin, **1991**.
- [32] An alternative mechanism, based on magnetic dipole–dipole interactions, has been sometimes invoked in order to explain the weak intermolecular magnetic interactions among organic radicals (see ref [1c]). This mechanism could explain the lack of statistically significant differences in the NO...ON and C–H...O contacts. Nevertheless, some studies indicate that the magnitude of magnetic dipolar interactions are much smaller than those originating from magnetic exchange interactions (see K. Takeda, K. Konishi, M. Tamura, M. Kinoshita, *Mol. Cryst. Liq. Cryst.* **1995**, *273*, 57).
- [33] Efforts in the theoretical and experimental directions are currently in progress in our laboratories in order to demonstrate unambiguously the validity of the McConnell-I model. Some of these studies are based on looking at the similarities in the patterns present in crystals showing similar magnetic properties. Another line of research is directed towards the theoretical basis of the McConnell-I model (M. Deumal, J. J. Novoa, M. J. Bearpark, P. Celani, M. Olivucci, M. A. Robb, *J. Phys. Chem. A* **1998**, *102*, 8404).

Received: August 3, 1998 [F1283]